Molecular Microbiology (2019) 112(1), 317–332

doi:10.1111/mmi.14272
First published online 20 May 2019

Snf2 controls pulcherriminic acid biosynthesis and antifungal activity of the biocontrol yeast *Metschnikowia pulcherrima*

Deborah Gore-Lloyd,[1†] Inés Sumann,[2†] Alexander O. Brachmann,[3] Kerstin Schneeberger,[4] Raúl A. Ortiz-Merino,[5] Mauro Moreno-Beltrán,[1] Michael Schläfli,[2] Pascal Kirner,[2] Amanda Santos Kron,[2] Maria Paula Rueda-Mejia,[2] Vincent Somerville,[4] Kenneth H. Wolfe,[5] Jörn Piel,[3] Christian H. Ahrens,[4,6] Daniel Henk[1‡] and Florian M. Freimoser[2*‡]

[1] *Department of Biology & Biochemistry, University of Bath, Bath, BA2 7AY, UK.*
[2] *Agroscope, Research Division Plant Protection, Müller-Thurgau-Strasse 29, 8820, Wädenswil, Switzerland.*
[3] *Institute of Microbiology, Eidgenössische Technische Hochschule (ETH) Zürich, 8093, Zürich, Switzerland.*
[4] *Competence Division Method Development and Analytics, Müller-Thurgau-Strasse 29, 8820, Wädenswil, Switzerland.*
[5] *Conway Institute, University College Dublin, Dublin 4, Ireland.*
[6] *SIB, Swiss Institute of Bioinformatics, Müller-Thurgau-Strasse 29, 8820, Wädenswil, Switzerland.*

Summary

Metschnikowia pulcherrima **synthesises the pigment pulcherrimin, from cyclodileucine (cyclo(Leu-Leu)) as a precursor, and exhibits strong antifungal activity against notorious plant pathogenic fungi. This yeast therefore has great potential for biocontrol applications against fungal diseases; particularly in the phyllosphere where this species is frequently found. To elucidate the molecular basis of the antifungal activity of *M. pulcherrima*, we compared a wild-type strain with a spontaneously occurring, pigmentless, weakly antagonistic mutant derivative. Whole genome sequencing of the wild-type and mutant strains identified a point mutation that creates a premature stop codon in the transcriptional regulator gene *SNF2* in the mutant. Complementation of the mutant strain with the wild-type *SNF2* gene restored pigmentation and recovered the strong antifungal activity. Mass spectrometry (UPLC HR HESI-MS) proved the presence of the pulcherrimin precursors cyclo(Leu-Leu) and pulcherriminic acid and identified new precursor and degradation products of pulcherriminic acid and/or pulcherrimin. All of these compounds were identified in the wild-type and complemented strain, but were undetectable in the pigmentless *snf2* mutant strain. These results thus identify Snf2 as a regulator of antifungal activity and pulcherriminic acid biosynthesis in *M. pulcherrima* and provide a starting point for deciphering the molecular functions underlying the antagonistic activity of this yeast.**

Accepted 5 May, 2019. *For correspondence. E-mail: florian.freimoser@agroscope.admin.ch; Tel. +41 58 460 6341; Fax. +41 58 460 6341.
†These authors share first authorship.
‡These authors share senior authorship.

Introduction

The yeast *Metschnikowia pulcherrima* is globally distributed and frequently isolated from the phyllosphere; in particular from flowers and fruits (Slavikova *et al.*, 2007; Pelliccia *et al.*, 2011; Vadkertiova *et al.*, 2012). Competition assays of 40 yeasts against a diverse set of 16 filamentous fungi identified *M. pulcherrima* as the overall strongest antagonist (Hilber-Bodmer *et al.*, 2017) and the same isolate was highly competitive against other antifungal yeasts on apples (Gross *et al.*, 2018). The species exhibits strong antagonistic activity against apple postharvest diseases caused by *Alternaria*, *Aspergillus*, *Botrytis, Fusarium, Monilinia* and *Penicillium* species (Piano *et al.*, 1997; Janisiewicz *et al.*, 2001; Spadaro *et al.*, 2002; Saravanakumar *et al.*, 2008; Turkel *et al.*, 2014; Ruiz-Moyano *et al.*, 2016) and was also identified as a potential biocontrol organism against foodborne pathogens of freshly cut apples (Leverentz *et al.*, 2006) as well as fungal grape diseases (De Curtis *et al.*, 2012; Parafati *et al.*, 2015). Besides fungal pathogens of fruits, *M. pulcherrima* also inhibits other yeasts (Oro *et al.*, 2014; Kántor *et al.*, 2015). In addition to biocontrol applications, *M. pulcherrima* is being considered for the synthesis of the fragrance molecule 2-phenylethanol (Chantasuban *et al.*, 2018), for biodegradation of the mycotoxin patulin (Reddy

et al., 2011) and for biofuel production (Santamauro *et al.*, 2014), and is being evaluated for the production of wines with lower alcohol content (Contreras *et al.*, 2014; Contreras *et al.*, 2015).

The designation 'the most beautiful' (translation of the Latin word '*pulcherrima*') *Metschnikowia* is based on the cells' uniform and spherical appearance in microscopic preparations (Kluyver *et al.*, 1953), and not the red pigment produced under certain growth conditions. However, the red pigment, forming spontaneously by a non-enzymatic reaction in the presence of iron under certain culture conditions, is a remarkable characteristic of *M. pulcherrima* colonies (Melvydas *et al.*, 2016). The compound responsible for this phenotype is described as pulcherrimin; an iron (III) chelate of pulcherriminic acid (2,5-diisobutyl-3,6-dihydroxy-pyrazine-1,4-dioxide). Pulcherriminic acid is formed by the oxidation of cyclodileucine (cyclo(Leu-Leu) (MacDonald, 1965; Uffen and Canale-Parola, 1972). Pulcherrimin was first described in yeasts more than 60 years ago, but only very recently the four genes involved in its biosynthesis and transport in *Kluyveromyces lactis* have been identified (Krause *et al.*, 2018), and the structure of the molecule synthesised by yeasts has not been determined by modern analytical methods. However, pulcherrimin is also produced by certain bacteria such as *Bacillus licheniformis*, where the two genes *yvmC* and *cypX*, coding for a cyclodipeptide synthase and cytochrome P450 oxidase, respectively, are responsible for its biosynthesis (Tang *et al.*, 2006; Gondry *et al.*, 2009; Cryle *et al.*, 2010). Expression of *yvmC* and *cypX* and the formation of pulcherrimin are intricately regulated by factors such as growth stage, iron availability or environmental stress (Randazzo *et al.*, 2016; Wang *et al.*, 2018). Iron chelation by pulcherriminic acid and formation of insoluble pulcherrimin, causing iron depletion in the growth substrate, is thought to mediate antimicrobial activity exhibited by some bacteria and yeasts (Sipiczki, 2006; Saravanakumar *et al.*, 2008; Wang *et al.*, 2018). However, alternative hypotheses to this mode of action cannot be excluded (e.g., antimicrobial activity due to precursors and independent of iron, regulatory effect on plant, fungal or bacterial responses, defence reaction against toxic iron levels) (Kluyver *et al.*, 1953; Sipiczki, 2006; Kántor *et al.*, 2015).

In the present study, we characterised the antifungal mode of action of *M. pulcherrima* by comparing pigmentless mutants with reduced antagonistic activity with their wild-type progenitor. Comparison of the mutants with the *de novo* assembled genome of the wild-type strain led to the identification of a premature stop codon in the transcriptional regulator *SNF2* as the cause for the observed phenotypes, which was confirmed by developing genetic tools and complementation of the mutant strain. We show by mass spectrometry (UPLC HR HESI-MS) that the *snf2* mutant neither synthesised detectable levels of pulcherriminic acid or cyclo(Leu-Leu), nor of any other precursor or degradation product thereof. This phenotype was likely caused by strongly reduced transcript levels of the pulcherrimin biosynthesis genes *PUL1* and *PUL2* (Krause *et al.*, 2018). These results establish the role of *M. pulcherrima SNF2* in the regulation of antagonistic activity and pulcherrimin biosynthesis. Our findings on pulcherrimin metabolism are not only biotechnologically relevant, but will allow further defining the mode of action of *M. pulcherrima*. Furthermore, the tools established in the course of this work open up new opportunities for application-oriented, fundamental research on the *M. pulcherrima* antifungal activity that will benefit phytopathology and the development of biocontrol solutions for important plant diseases.

Results

Naturally occurring, pigmentless M. pulcherrima *mutants are less antagonistic than the wild type*

Based on the original literature, *M. pulcherrima* synthesises pulcherriminic acid from cyclodileucine (MacDonald, 1965). In the presence of iron (III), a non-enzymatic reaction converts pulcherriminic acid into the red pigment pulcherrimin. Pigmentless, white mutants have previously been reported after nitrosoguanidine treatment (Sipiczki, 2006). Here, such mutants were found to occur spontaneously among freeze-dried cells of a yeast species identified as *M.* aff. *pulcherrima* (hereafter, *M. pulcherrima*) that were stored at 22°C for several months. Since pulcherrimin has been implicated in the antagonistic activity of *M. pulcherrima* and *Bacillus licheniformis*, supposedly due to its iron immobilising activity (Sipiczki, 2006; Wang *et al.*, 2018), we characterised pigmentless *M. pulcherrima* mutants with respect to their antagonistic activity against plant pathogenic fungi.

The *M. pulcherrima* wild-type isolate APC 1.2 (WT) exhibited increased pigmentation with increasing iron concentrations, while the mutant cells (isolate W8) remained pigmentless (white) irrespective of the iron concentration in the growth medium (Fig. 1A). Phenotypic microarrays (Biolog YT MicroPlates™) confirmed the limited metabolic versatility of the *M. pulcherrima* WT APC 1.2 (Hilber-Bodmer *et al.*, 2017) and did not suggest broad differences between the strains (Supplementary Figure S1). Binary competition assays on potato dextrose agar (PDA) plates (Fig. 1B) confirmed strong inhibition of the plant pathogenic fungus *Botrytis caroliniana* by the *M. pulcherrima* WT (98% reduction in the growth area as compared to a control growing in the absence of the yeast) (Fig. 1C). In contrast, the *M. pulcherrima* pigmentless mutant W8 inhibited *B. caroliniana* less than the wild type (80% reduction of the growth area). This

reduced antifungal activity of the non-pigmented mutants was similarly observed in competition assays against *Gibberella fujikuroi* and *Fusarium oxysporum* (56% and 45% vs. 89% and 81% reduction) and with two other, independent, pigmentless *M. pulcherrima* mutants W10 and W11 (37%–51% reduction vs. 75% reduction by the wild type) (Supplementary Figure S2). The strong antagonistic activity of the *M. pulcherrima* WT and the reduced

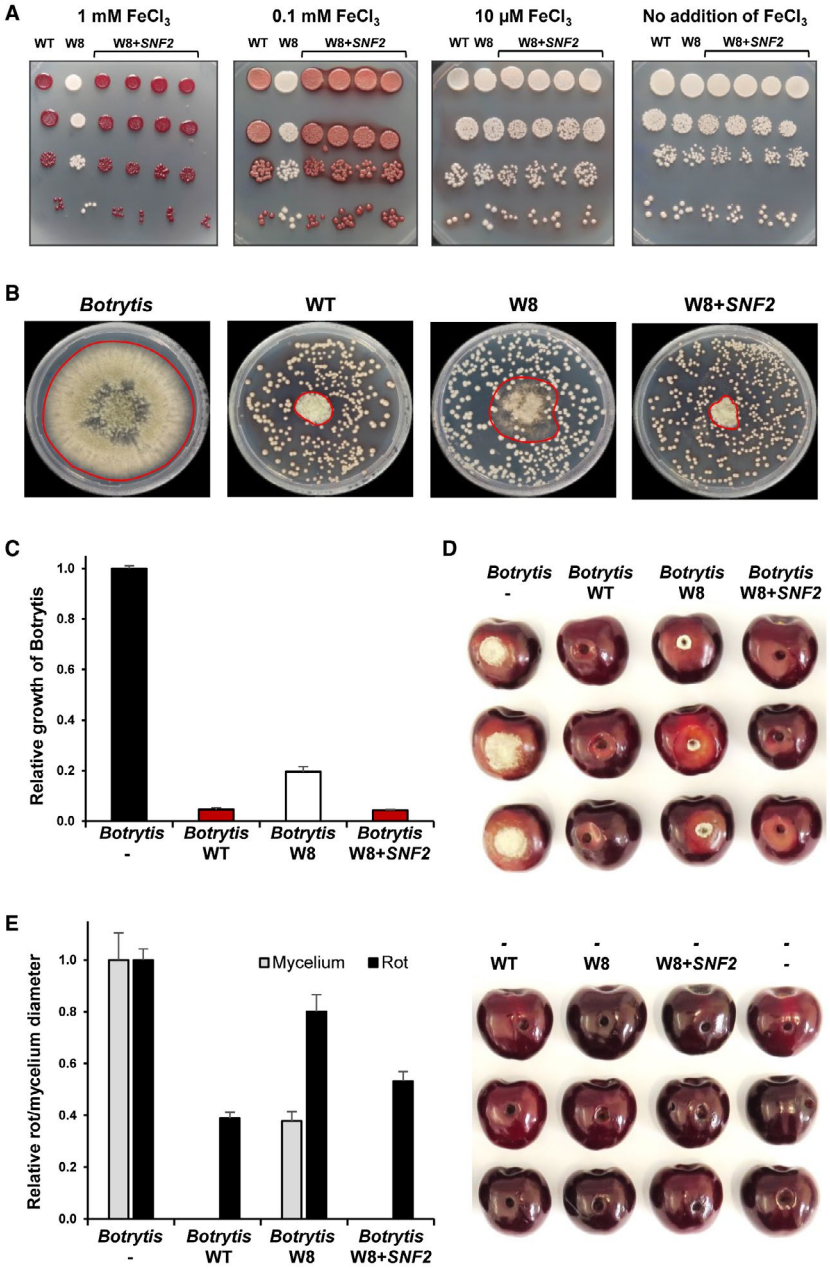

Fig. 1. Complementation with *SNF2* restores pulcherrimin biosynthesis and antagonistic activity in a pigmentless *M. pulcherrima* mutant. All experiments were performed with the *M. pulcherrima* wild-type (WT; isolate APC 1.2), mutant (W8) and complemented (W8 + *SNF2*) strains. A. The pigmentless *M. pulcherrima* mutant (W8, second column) remained white irrespective of the amount of iron (III) ($FeCl_3$; 0–1 mM) added to the growth medium, while the wild-type (WT, first column) and four complemented strains (columns 3–6) showed strong pigmentation, indicative of pulcherrimin biosynthesis, if grown in medium supplemented with at least 100 µM $FeCl_3$. B. C. Binary competition assays against *Botrytis* (*B. caroliana*; isolate EC 1.05, SH177344.07FU) were performed on PDA plates and the relative growth area, as compared to the wild type, was quantified. The area occupied by *Botrytis* mycelium is marked in the photograph and the data in the histogram show the means and standard errors of four replicates. D. E. Bioassays with freshly harvested, conventionally grown cherries were performed with *Botrytis* as the plant pathogen. The diameter of the *Botrytis* mycelium developing around the artificially introduced lesion, as well as the (larger) diameter of the rot (lighter coloured, sunken area around the lesion) were measured. The *M. pulcherrima* wild-type and complemented strains abolished the formation of *Botrytis* mycelium around the lesion. None of the yeasts alone, without *Botrytis*, caused rot or mycelium development on the cherries.

antifungal effect of the W8 mutant were confirmed in bioassays on cherries that were infected with *B. caroliniana* (Fig. 1D). Compared to cherries infected with the plant pathogen alone, the *M. pulcherrima* WT strongly suppressed *Botrytis* on cherries with respect to rot diameter and abolished mycelium development (Fig. 1E). In contrast, the W8 mutant only weakly suppressed *Botrytis*, leading to strongly increased rot diameter and mycelium development of *B. caroliniana,* albeit in lower frequency and less profusely than in the cherries only inoculated with *Botrytis* (1D and E). Overall, these results demonstrated reduced (but still detectable) antifungal activity of the pigmentless, white *M. pulcherrima* mutant W8 *in vitro* as well as in cherries.

Pigmentless M. pulcherrima *mutants do not secrete cyclodileucine or pulcherriminic acid*

The white *M. pulcherrima* mutant seemed to lack the red pigment pulcherrimin, but it was not clear if the pigment produced by our *M. pulcherrima* isolate APC 1.2 indeed corresponded to the compound described as pulcherrimin, if the precursors cyclo(Leu-Leu) and/or pulcherriminic acid were not synthesised, or if another defect prevented the formation of the iron chelate. Therefore, we analysed the culture supernatants of wild-type and mutant *M. pulcherrima* cells by ultra-performance liquid chromatography-high resolution heated electrospray ionisation mass spectrometry (UPLC HR HESI-MS) in order to identify the soluble pulcherrimin precursors cyclo (Leu-Leu) and pulcherriminic acid.

High-resolution MS measurements in combination with ^{15}N- and ^{13}C-labelling experiments allowed determining the molecular formulas of several dipeptides. Metabolites secreted by the *M. pulcherrima* WT and W8 mutant during growth were absorbed with Amberlite® XAD16 resin and extracts thereof were analysed by UPLC HR HESI-MS. We identified at least five dipeptides that were secreted by *M. pulcherrima* WT cells, but were not detected in the W8 mutant supernatants (Fig. 2A). Comparison with a cyclo(Leu-Leu) standard identified **1** as cyclo(L-leucyl-L-leucyl) (Supplementary Figure S3). Extensive UPLC HR HESI-MS analyses, including reverse stable isotope labelling with L-leucine, L-isoleucine and L-valine in a ^{13}C-background, confirmed the incorporation of two L-leucine into all five compounds (Fig. 2, Supplementary Figure S4). Based on these analyses, **2** was identified as pulcherriminic acid and **3** might represent a di-*N*-hydroxylated intermediate of **1** (Fig. 2, Supplementary Figure S4). The molecular formula of **4** suggests an additional hydroxylation of **2** and also ring opening, whereas **5** indicates a decarboxylation event due to the incorporation of only one C_6- and one C_5-L-leucine derived carbon backbone, instead of two C_6- carbon skeletons. In this respect, **5** might represent a degradation product of **4** (Fig. 2B). Besides that, we observed two C_4-backbones in all compounds after L-valine supplementation. Here, valine is likely metabolised via 2-isopropylmalate into leucine before incorporation (Fig. 2, Supplementary Figure S4). Based on our results, we identified three of these compounds as the pulcherrimin precursors cyclo(L-leucyl-L-leucyl), pulcherriminic acid, and a yet uncharacterised precursor or shunt product, while the other two compounds likely represent novel degradation products.

Pigmentless M. pulcherrima *mutants harbour a point mutation leading to a premature stop codon in the gene encoding the transcriptional regulator Snf2*

In order to identify the underlying genetic mutations leading to the lack of cyclodipeptide biosynthesis and weakly antagonistic *M. pulcherrima* phenotype, a high-quality reference genome for the *M. pulcherrima* wild-type strain APC 1.2 was *de novo* assembled relying on long-read PacBio sequencing.

The final, assembled and annotated genome (assembly with Canu (Koren *et al*., 2017), 254× average coverage, N50 > 2.5 million bp) indicated a genome size of 15.88 Mbp, a G + C content of 46% and 5800 protein-coding genes (Table 1). Based on the high coverage and completeness of this assembly, it may become a reference genome for *M. pulcherrima*. The genome contains two genes for tRNA-Ser(CAG)(MPUL0Etrna0S and MPUL0Ftrna0S), consistent with a CUG-Ser genetic code as expected for this species, which is relatively closely related to *Candida albicans*. The nuclear genome was assembled into seven large scaffolds (>600 kb). Six of the 14 ends of these 7 scaffolds terminated at 18S or 26S ribosomal RNA genes, and the others terminated at putative subtelomeric repeats that were shared among scaffold ends. These seven scaffolds were considered representing full chromosomes and are thus referred to as such. The 5S rRNA genes are dispersed at many locations around the genome, as in *M. bicuspidata* (Riley *et al*., 2016). The distribution of empirical allele frequencies from single nucleotide variants found after mapping of Illumina data to the PacBio assembly (Ortiz-Merino *et al*., 2018) indicated that the wild-type strain studied here (APC 1.2) is neither diploid nor a hybrid, in contrast to the other reported genome sequences of strains from the *M. pulcherrima/M. fructicola* subclade that are highly heterozygous and probably interspecies hybrids (Venkatesh *et al*., 2018; Piombo *et al*., 2018; Sipiczki *et al*., 2018).

In order to identify the genetic mutations in the pigmentless *M. pulcherrima* mutant, Illumina HiSeq reads of the three pigmentless mutants W8, W10 and W11 (originating from three individual colonies after plating the same batch of freeze-dried *M. pulcherrima* cells that was stored at 22 °C for several months) were generated and mapped to

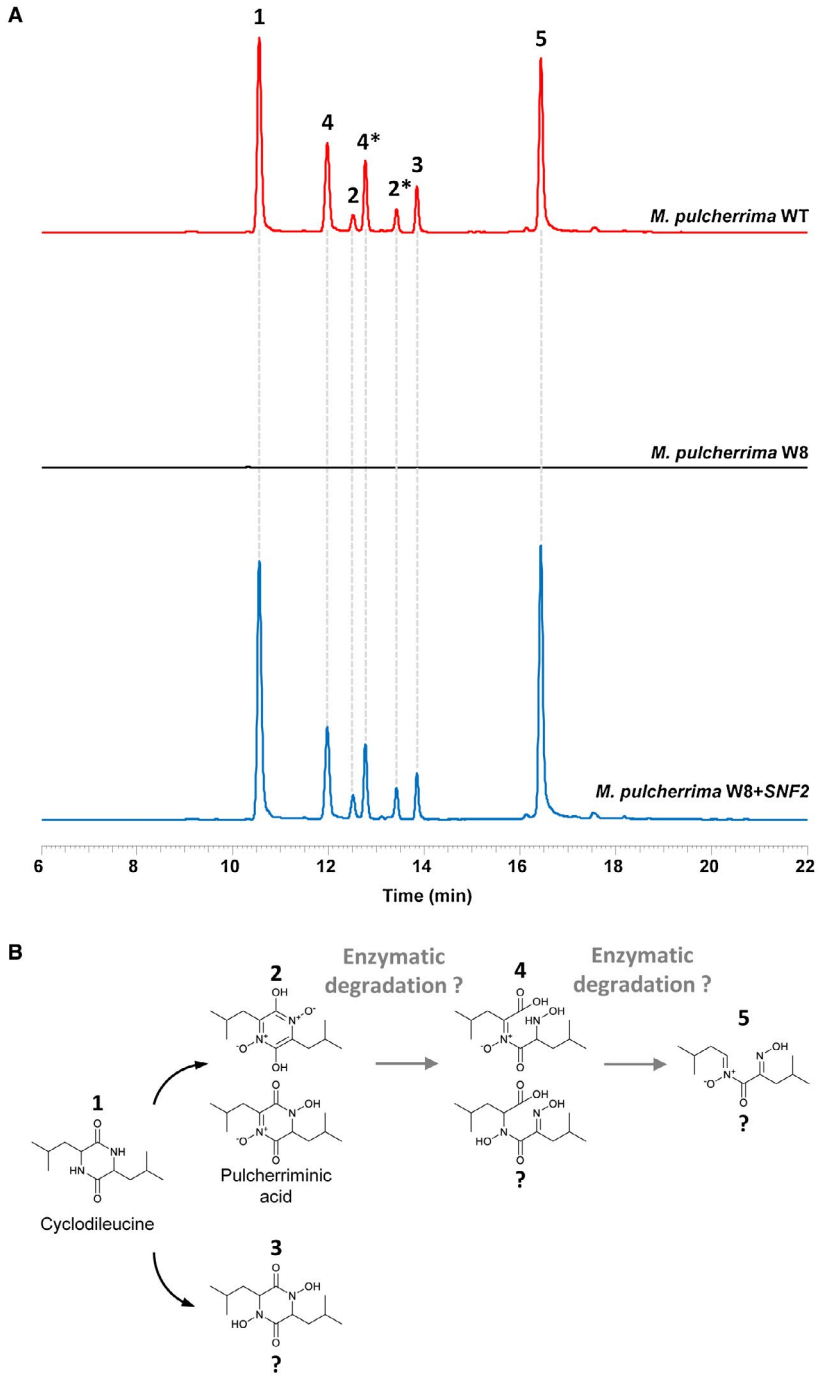

Fig. 2. A pigmentless *M. pulcherrima* mutant does not secrete cyclic dipeptides.
A. UPLC HR HESI-MS metabolic profiles for (1, cyclo(Leu-Leu), 227.176 m/*z* $[M + H]^+$, $C_{12}H_{22}N_2O_2$) derived derivatives in the wild type of *M. pulcherrima* (red), *snf2* mutant (black) and a *SNF2* complemented mutant (blue). (2, pulcherriminic acid, 257.150 m/*z* $[M + H]^+$, $C_{12}H_{20}N_2O_4$), (3, 259.165 m/*z* $[M + H]^+$, $C_{12}H_{22}N_2O_4$), (4, 275.161 m/*z* $[M + H]^+$, $C_{12}H_{22}N_2O_5$), (5, 229.155 m/*z* $[M + H]^+$, $C_{11}H_{20}N_2O_3$). Potential tautomers are marked with an asterisk.
B. Proposed structures for **1** cyclo(Leu-Leu)-derived metabolites. **2** pulcherriminic acid and **3** are precursors for pulcherrimin. In contrast and based on our feeding experiments, **4** and **5** might represent so far undescribed degradation products of **2**. [Colour figure can be viewed at wileyonlinelibrary.com]

our *M. pulcherrima* reference genome. The only mutation that was identically detected in all three mutants was a C → A point mutation leading to a premature stop codon at position 1262 of the *MPUL0C08850* gene (Supplementary Table S1). This gene encodes an ortholog of *S. cerevisiae SNF2* (Fig. 3A) and its product is hereafter named

Table 1. Assembly and genome statistics for *M. pulcherrima*, *M. fructicola* and *M. bicuspidate*.

	M. pulcherrima	***M. fructicola***	***M. bicuspidata***
Technology	**PacBio**	PacBio	454, Illumina
Assembler	**Canu**	HGAP 3.0	Newbler v2.5
Coverage (x)	**254**	20	16
Assembly (Mbp)	**15.88**	24.48	16.06
Contigs (n)	**7**	93 (93 scaffolds)	421 (33 scaffolds)
N_{50} (bp)	**2′688′338**	957′836	62′344
GC (%)	**46**	46	47
Proteins (n)	**5800 (genes)**	NA	5,851
tRNAs (n)	**227**	NA	NA

The statistics refer to the *Metschnikowia bicuspidata* NRRL YB-4993 (35) and *M. fructicola* strain 277(38) genomes. For *M. pulcherrima*, the seven scaffolds refer to the nuclear genome (excluding the mitochondrial genome).

The statistics for the *M. pulcherrima* genome presented here are shown in bold.

METSCH-Snf2 (Fig. 3A). The identified point mutation predicted to result in a truncated METSCH-Snf2 protein of 420 amino acids in length, as compared to 1578 amino acids for the full-length protein, that lacked all domains and motifs except for the first glutamine-leucine-glutamine (QLQ) domain (Supplementary Figure S5). The functionally relevant helicase and bromo domains (Laurent *et al.*, 1993b) were thus not present in the METSCH-Snf2 protein of the *M. pulcherrima* mutants tested here, which likely resulted in a non-functional Snf2 protein.

In summary, we *de novo* assembled a high-quality reference genome for *M. pulcherrima* that served as the basis for identifying a single point mutation in pigmentless mutants exhibiting reduced antagonistic activity. An identical point mutation was found in three pigmentless strains, indicating that it likely arose by a single mutation event. The point mutation introduced a premature stop codon in *MPUL0C08850* (*snf2*), which resulted in a truncated METSCH-Snf2 protein and likely caused a complex phenotype including reduced antifungal activity and lack of cyclodipeptide synthesis.

Pigmentless M. pulcherrima *mutants exhibit strongly reduced PUL gene transcription and broad transcriptional changes across the entire genome*

Since Snf2 acts as a transcriptional regulator in *S. cerevisiae*, we expected that the *snf2* mutation in the pigmentless *M. pulcherrima* mutants may interfere with transcription of the clustered *PUL* genes that were recently identified to confer pulcherrimin biosynthesis and utilisation in *K. lactis* (Krause *et al.*, 2018). Using the *PUL* gene products identified by Krause *et al.* (2018), the *M. pulcherrima* homologs were readily identified as *MPUL0C04990* (*PUL1*; 31% identity at the protein level with *K. lactis* KLLA0_C19184g), *MPUL0C04980* (*PUL2*; 50% identity with KLLA0_C19206g), *MPUL0C04960* (*PUL3*; 45% identity with KLLA0_C19250g) and *MPUL0C04970* (*PUL4*; 32% identity with KLLA0_C19228g).

A comparison of the RNAseq data from *M. pulcherrima* wild-type and W8 *snf2* mutant cells confirmed broad transcriptional changes and the *PUL* genes were among the most strongly downregulated transcripts (Fig. 3B). Besides transcript counts for the *PUL* genes, most candidapepsin genes (secreted aspartic proteases (SAP), four out of five transcribed genes; six SAP genes in total), several transporters (e.g., iron, sugar and MFS-type transporters), as well as genes encoding proteins with various functions (e.g., mannosyltransferase, ribonuclease, acetyltransferase, uridylyltransferase, decarboxylase, CheY chemotaxis protein, LicD family protein) and hypothetical proteins were significantly less transcribed in the W8 mutant as compared to the WT under the conditions tested here (Fig. 3B). The transcriptional changes were not limited to the *PUL* gene cluster or a specific region of the genome, but broadly affected all seven nuclear chromosomes (Fig. 3C). In the W8 *snf2* mutant, the transcript counts for *PUL1*, *PUL2* and *PUL3* were over 100-fold reduced (2000-fold for *PUL2*), while *PUL4*, encoding a putative transcriptional regulator of the *PUL* genes, was generally lowly transcribed and less affected by the *snf2* mutation (Fig. 3D).

These transcript analyses suggest that the complex phenotype of reduced antifungal activity, exhibited by the pigmentless *M. pulcherrima* cells harbouring a *snf2* mutation, was likely due to a broadly altered transcriptional profile and in particular, with respect to pigmentation, severely downregulated *PUL* gene transcription.

Complementation of pigmentless M. pulcherrima *mutants with* SNF2 *restores antagonistic activity and cyclodipeptide synthesis*

To test in an independent experiment whether the premature stop codon in the mutant *snf2* gene was responsible for the lack of pulcherrimin production and the reduced antagonistic activity, a transformation protocol for *M. pulcherrima* was established and the *M. pulcherrima* wild-type *SNF2* gene was reintroduced into the W8

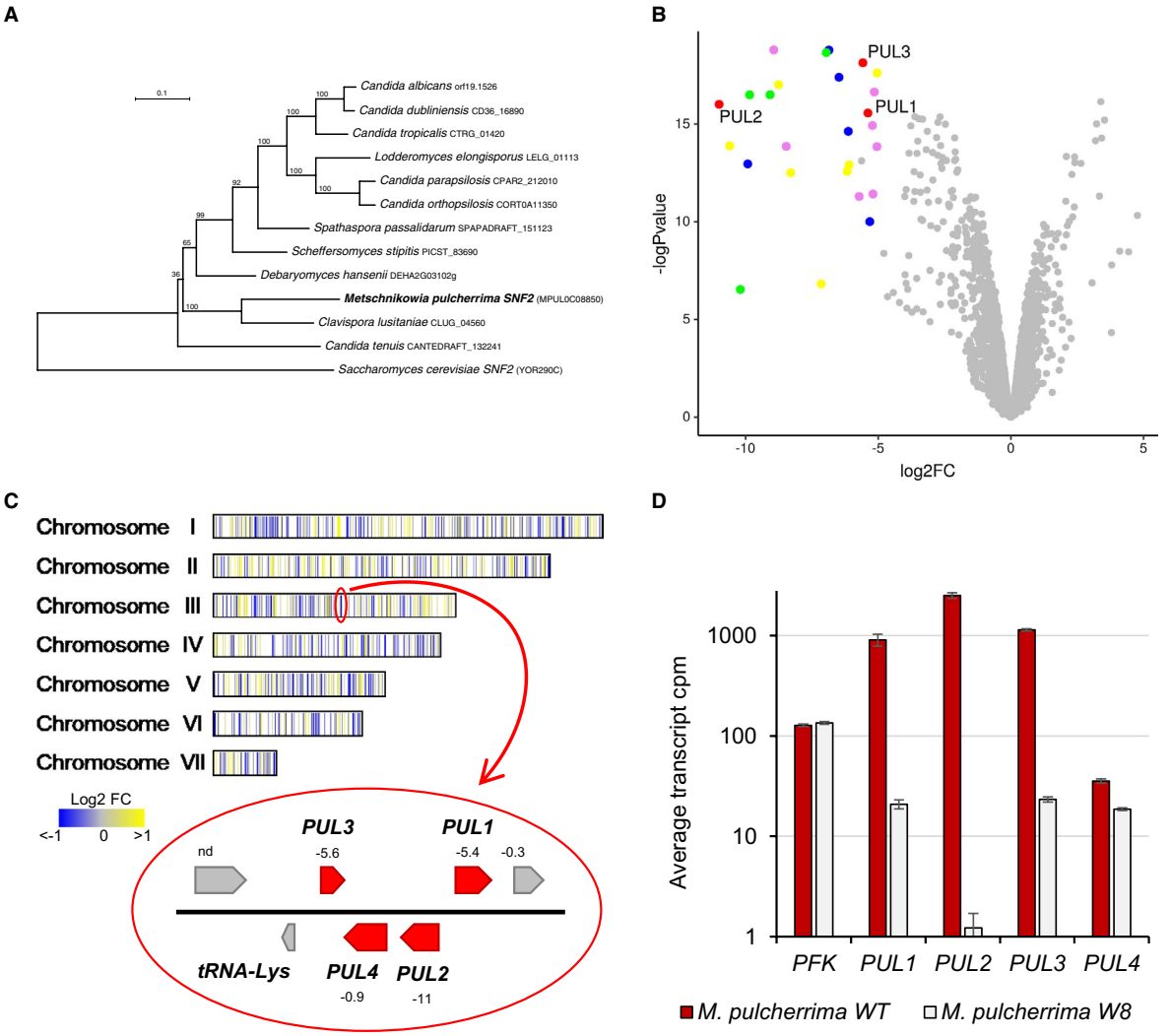

Fig. 3. Pigmentless *M. pulcherrima* mutants exhibit strongly reduced *PUL* gene transcription and broad transcriptional changes across the entire genome.
A. Phylogenetic relationship of *M. pulcherrima* Snf2 protein to its orthologs in other CUG-Ser clade species, with *S. cerevisiae* Snf2 as outgroup. The tree was constructed by maximum likelihood, and bootstrap supports for internal branches are shown.
B. Volcano plot of the fold changes for all genes in *snf2* mutant versus wild-type cells. The *x*-axis represents the log2 fold change between the mutant and wild type, while the negative log10 of the P-value of is indicated on the *y*-axis. The genes most strongly downregulated in the mutant are labelled by colours: *PUL* genes (), genes encoding candidapepsins (), transporters (), other functions (), or hypothetical proteins () and all other genes ().
C. Schematic representation of the seven nuclear chromosomes and the distribution of the transcriptional changes in the *snf2* mutant as compared to the WT strain. Blue: downregulated genes, yellow: upregulated genes; white: genes with a p-Value and/or FDR > 5%. The *PUL* gene cluster is located on chromosme III and comprised three of the most strongly downregulated genes (*PUL 1-3*). D. The *M. pulcherrima* wild-type (red) and W8 snf2 mutant cells (white) exhibited strongly reduced transcript counts for *PUL1* (*MPUL0C04990*), *PUL2* (*MPUL0C04980*) and *PUL3* (*MPUL0C04960*), while the *PUL4* gene (*MPUL0C04970*), encoding a putative transcriptional regulator of the *PUL* genes, was generally lowly transcribed and less affected by the snf2 mutation. As a reference, transcript counts for the 6-phosphofructo-2-kinase (*MPUL0A12740*) are shown. The values represent mean transcript counts and the standard error of two and three samples for the wild type and the mutant respectively.

mutant strain by random integration into the genome (Supplementary Figure S6).

Transformation of W8 with a construct containing the METSCH-Snf2 coding gene *MPUL0C08850* under its native promoter, along with a nourseothricin resistance gene selection marker, resulted in pigmented colonies, while transformation with the *snf2* allele did not recover the red phenotype (Supplementary Figure S6). Among 30 transformants growing on the nourseothricin plates, 23 strains exhibited a stable, red phenotype, 5 strains were unstable and showed red and white colonies after several subculturing rounds, and 2 strains showed the original

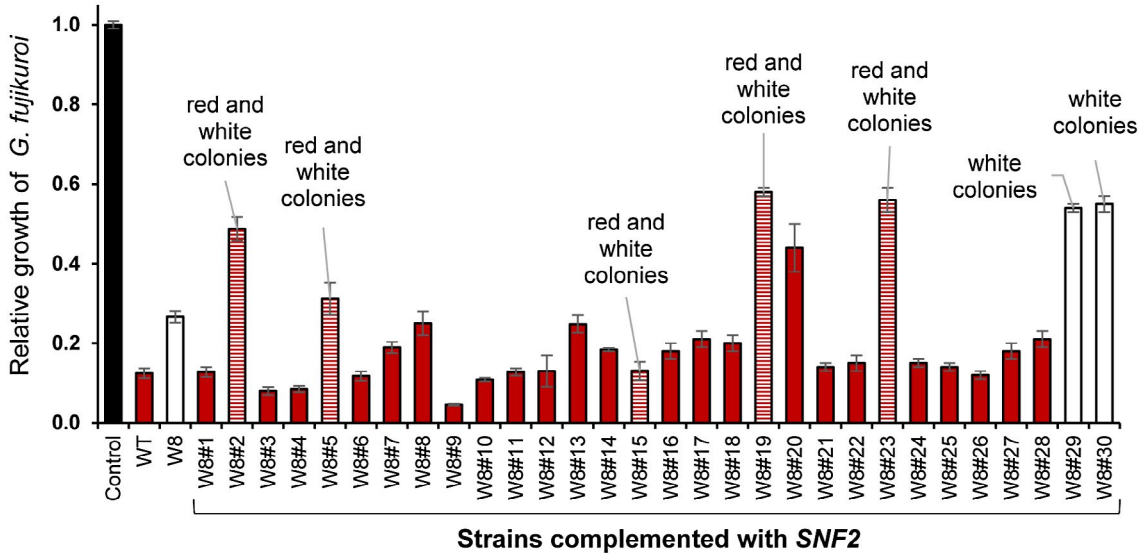

Fig. 4. The majority of the complemented strains exhibited a stable, red phenotype and restored antifungal activity. Thirty complemented *M. pulcherrima* strains, the original wild type (APC 1.2) and the pigmentless mutant W8 were tested in binary competition assays against the plant pathogenic fungus *G. fujikuroi*. Growth of *G. fujikuroi* in the presence of the different complemented strains is shown relative to growth in the absence of yeasts (control bar). The colour of the bars indicates pigmentation of the wild-type and the complemented strains. In all cases, the mean relative growth of four replicates and the standard error are shown.

white phenotype (Fig. 4). Almost all complemented, red strains restored antifungal activity against *G. fujikuroi* to comparable levels as observed for the wild type (Fig. 4). The complemented strain #12 was analysed in more detail by growth experiments, competition assays against plant pathogenic fungi, bioassays on cherries and UPLC HR HESI-MS analysis of the metabolites secreted during growth in PDB.

Pigmentation of the complemented *M. pulcherrima* strain W8#12 on agar plates with increasing iron concentrations was similar to the wild type and remained stable (Fig. 1A). The antagonistic activity was also restored to wild-type levels, as indicated by binary competition assays on agar plates against *B. caroliniana*, *G. fujikuroi* and *F. oxysporum* isolates (1B and C; Supplementary Figure S2A). Likewise, on cherries, the complemented *M. pulcherrima* mutant W8#12 showed restored antagonistic activity both with respect to rot diameter and mycelium development in artificially wounded and infected cherry fruits (1D and E). Finally, introduction of the wild-type *SNF2* gene restored the secretion of **1**, cyclo(L-leucyl-L-leucyl), **2**, pulcherriminic acid, as well as an unidentified precursor **3** and two probable degradation products **4** and **5,** into the culture supernatants of the complemented strain #12 (Fig. 2A). Overall, these results defined a point mutation in the METSCH-Snf2 coding gene *MPUL0C08850* as the underlying cause for abolished pigmentation, lack of pulcherriminic acid secretion and reduced antagonistic and biocontrol activity against plant pathogenic fungi.

Discussion

M. pulcherrima is a strongly antifungal yeast that is frequently identified in the phyllosphere and considered a promising species for biocontrol applications. Its most prominent characteristic is the formation of a red pigment, pulcherrimin, that was discovered over 60 years ago (Kluyver *et al.*, 1953). This compound represents an insoluble complex of iron and pulcherriminic acid that forms non-enzymatically in the presence of iron III (Kluyver *et al.*, 1953; Cook and Slater, 1954; MacDonald, 1963; MacDonald, 1965; Uffen and Canale-Parola, 1972). Pulcherrimin formation may serve as a defence against deleterious effects of high amounts of iron (reviewed by Kluyver *et al.* (1953)) and is thought to deprive competing microbes of iron and thus limit their growth (Sipiczki, 2006; Saravanakumar *et al.*, 2008; Kántor *et al.*, 2015; Li *et al.*, 2017; Wang *et al.*, 2018). Although pulcherrimin levels and antifungal activity seem to correlate, as suggested previously (Sipiczki, 2006) and shown here by quantitative competition assays with pigmentless and complemented mutants, a causal relationship between iron deprivation by pulcherrimin and antifungal activity has not been demonstrated. The function of pulcherrimin has thus not been elucidated in detail yet and the role of iron and iron chelation is not resolved. For example, pulcherriminic acid is also synthesised under iron replete conditions, which is the reason why antimicrobial activities irrespective of iron or iron monopolisation, rather than iron scavenging, have also been hypothesised as

modes of action (Sipiczki, 2006; Krause *et al*., 2018; Kupfer *et al*., 1967). It has also been observed that the addition of iron may, in some cases, increase or at least not significantly diminish antifungal activity (Piano *et al*., 1997; Saravanakumar *et al*., 2008), which would not be expected if iron depletion was the mode of action. While a recent study identified a putative transporter enabling yeast to take up and utilise pulcherrimin as a proper siderophore (Krause *et al*., 2018), it has also been doubted whether or not iron can be taken up from the insoluble pulcherrimin complex and serve as an iron source for the synthesising organisms (e.g., bacteria and yeasts) (Wang *et al*., 2018). In *Bacillus subtilis,* where pulcherrimin biosynthesis has been studied in more detail, the formation of the pulcherrimin precursor pulcherriminic acid does not depend on iron availability and the main repressor of pulcherriminic acid biosynthesis (YvmB) is even upregulated under iron starvation (Kupfer *et al*., 1967; Randazzo *et al*., 2016), also arguing against a role of pulcherrimin in iron provision. It has therefore been suggested that iron chelation by pulcherriminic acid may interfere with iron-dependent cellular process in general and thereby indirectly cause diverse changes in the cell (Randazzo *et al*., 2016).

The study presented here was initiated by the discovery of spontaneously occurring, pigmentless *M. pulcherrima* mutants. The pigmentless phenotype was regularly observed after plating freeze-dried cells that had been stored at 22°C for several months (but not in cells stored at 4°C); at a time point when the viability of the stored cells had already strongly diminished (in contrast to the cells stored at 4°C, which remained viable). Under the standard growth and assay conditions used throughout the studies shown here, the pigmentless *M. pulcherrima* mutants did not exhibit any growth defect; if anything, the mutants grew better, as could be expected based on the lack of an antimicrobial metabolite. In general, the *snf2* METSCH strain did not exhibit an apparent growth phenotype and its metabolic profile was similar to the wild type (as analysed by Biolog YT MicroPlates™; Supplementary Figure S1). The lack in pigmentation and reduced antifungal activity were thus the most prominent and reliably detected phenotypes of the *snf2* mutant cells.

The red pigment pulcherrimin has caught the interest of research already more than 60 years ago, but much about its chemical nature, synthesis and biological function remains to be elucidated. Here, we formally prove the presence of cyclo(L-leucyl-L-leucyl) and four congeners, including the pulcherrimin precursor pulcherriminic acid. UPLC HR HESI-MS in combination with labelling and feeding experiments provided not only exact molecular formulas, but also biosynthetic information that allowed us to identify two possible degradation products of pulcherriminc acid or pulcherrimin. These products may arise from enzymatic reactions involving monooxygenation and decarboxylation, but the exact mechanism still has to be elucidated. In addition, it is not yet clear if these new intermediates and possible degradation products contribute to the overall antifungal activity of *M. pulcherrima* and what the biological function of pulcherriminic acid/pulcherrimin degradation is.

Although the reduced antifungal activity of the pigmentless *M. pulcherrima* cells supports the notion that pulcherrimin may indeed be responsible for the suppressive phenotype, it is important to note that pigmentless mutants only showed reduced antifungal activity and still strongly inhibited the growth of filamentous fungi. In comparison to the antifungal activities of a broad collection of 40 different yeasts (Hilber-Bodmer *et al*., 2017), the inhibition caused by the pigmentless *M. pulcherrima* mutant reported here was still among the strongest of all the yeasts tested. This is in contrast to findings by Sipiczki, who reported lack of antifungal activity in nitrosoguanidin-generated, pigmentless *M. pulcherrima* mutants (Sipiczki, 2006). However, it is important to note that in the latter study undefined, chemically induced mutants were used (that likely harbour multiple different mutations) and inhibition zones of a few millimetres in size were measured, while in the present work growth areas (in the range of ca. 0–2000 mm^2) of the filamentous fungus in presence of defined amounts of yeasts (with only one mutation) were determined (Hilber-Bodmer *et al*., 2017). The seemingly conflicting results obtained with the different pigmentless *M. pulcherrima* mutants may thus be due to differences in the nature of the mutants themselves as well as in the types of competition assays that were used in the two studies. The results presented here clearly demonstrate that the *M. pulcherrima* antifungal activity depends on several factors, which may explain the lack of reliable antifungal activity of *M. pulcherrima* culture supernatants containing pulcherrimin and pulcherriminic acid. The nature and interplay of the mechanisms contributing to *M. pulcherrima* antifungal activity, including pulcherrimin formation, are thus still largely unknown and need to be studied and elucidated in much more detail.

By exclusively relying on long PacBio reads, we were able to *de novo* assemble a high-quality reference genome of the *M. pulcherrima* WT strain APC 1.2. Mapping the genome sequences of mutant strains against it allowed us to readily identify the mutation that causes the pigmentless phenotype in *M. pulcherrima*: the homolog of the *S. cerevisiae SNF2* gene was affected by a point mutation that caused a premature stop codon and thus encoded for a truncated METSCH-Snf2 protein. In *S. cerevisiae*, Snf2 is a non-essential ATPase that modulates nucleosome structure as part of the SWI/SNF chromatin remodelling complex and thus regulates transcription of a plethora of genes (Laurent

et al., 1993a; Peterson and Tamkun, 1995; Dutta *et al.*, 2017). The gene/protein name is derived from the sucrose non-fermenting phenotype (Carlson *et al.*, 1981; Neigeborn and Carlson, 1984), but *SNF2* deletion and mutations strongly affect yeast metabolism overall (Mulleder *et al.*, 2016) and cause a diverse range of phenotypes including abolished mating type switching and sporulation, decreased resistance (e.g., to chemicals, metals, killer toxin), or altered cytosolic pH (Stern *et al.*, 1984; Enyenihi and Saunders, 2003; Dudley *et al.*, 2005; Chai *et al.*, 2005; Orij *et al.*, 2012; Serviene *et al.*, 2012). In humans, mutations in the *SNF2* homolog, and components of the SWI/SNF complex in general, are frequently identified in different types of cancers, leukaemia and other disorders (Wilson and Roberts, 2011; Biegel *et al.*, 2014; Prasad *et al.*, 2015; Agaimy and Foulkes, 2018). In this study, a point mutation leading to a premature stop codon in the METSCH-Snf2 coding gene *MPUL0C08850* caused a pigmentless phenotype by abolishing cyclodipeptide synthesis (i.e., synthesis of cyclo(Leu-Leu) and pulcherriminic acid) and reduced antifungal activity as demonstrated by competition assays on plates and bioassays on fruits against plant pathogenic fungi. Our results thus link Snf2 activity to the regulation of pulcherrimin metabolism and antifungal activity. This was confirmed by the strongly reduced transcript levels of the recently identified pulcherrimin biosynthesis genes *PUL1* (*MPUL*0C04990) and *PUL2* (*MPUL*0C04980) in the *snf* mutant strain as compared to the wild type. *PUL4* transcript levels, on the other hand, were hardly affected by the *snf2* mutation, which may seem surprising since this gene was identified as a transcriptional regulator (Krause *et al.*, 2018). However, Snf2 is part of a chromatin remodelling complex that regulates nucleosome structure (Liu *et al.*, 2017) and thus does not act as a transcription factor itself. The lack of Snf2 may prevent chromatin remodelling at the *PUL1*, *PUL2* and *PUL3* loci and thereby prevent efficient transcription of the corresponding genes irrespective of the presence of *PUL4*. Although the four *PUL* genes are clustered, the *snf2* mutation thus seems to cause differential effects on their transcription. This finding fits the overall pattern of up- and down-regulation: the mutation in the chromatin remodeller METSCH-Snf2 resulted in a broadly changed transcriptional profile across the entire genome that was characterised by confined regions of up- and down-regulation that were spread over all seven chromosomes. In addition to the *PUL* genes, other genes encoding proteins that may contribute to the antifungal activity of *M. pulcherrima* were strongly downregulated in the *snf2* mutant. These included, for example, genes encoding secreted proteases or different types of transporters; functions which were already implicated in biocontrol activity of other yeasts (Bar-Shimon *et al.*, 2004; Banani *et al.*, 2014; Laur *et al.*, 2018). The reduced antifungal activity of the *M. pulcherrima snf2* mutant (growth reduction of a plant pathogenic fungus from 98% to 80%) is thus likely not only due to the lack of pulcherrimin, but the result of altered levels (down-regulated, but for some genes possibly also increased levels) of different factors contributing to the complex biocontrol phenotype.

In summary, this multidisciplinary study identified a point mutation in the METSCH-Snf2 coding gene *MPUL0C08850* as the underlying cause for lack of pigmentation, abolished cyclodipeptide biosynthesis, and reduced antifungal activity. The identification of METSCH-Snf2 as a regulator of pulcherriminic acid biosynthesis and antifungal activity thus serves as a starting point and enabler for further elucidating pulcherrimin metabolism and function in *M. pulcherrima*, which will hopefully benefit biocontrol applications of this yeast in the future.

Experimental procedures

Isolates, species identification and cultivation

All isolates were initially identified by PCR and sequencing the ITS region of rDNA and assigning a UNITE species hypothesis (Abarenkov *et al.*, 2010; Hilber-Bodmer *et al.*, 2017; Nilsson *et al.*, 2018). The wild-type isolate APC 1.2 (CCOS978; Culture Collection of Switzerland) was originally isolated from apple flowers in Switzerland (Hilber-Bodmer *et al.*, 2017) and was assigned to UNITE SH180747.07FU, corresponding to *M. pulcherrima* (Pitt & M.W. Mill.). Subsequent phylogenetic analysis of the eight ITS regions present in the rDNA loci of its genome sequence indicated that, like *M. fructicola* and *M. andauensis*, strain APC 1.2 contains multiple diverse ITS sequences that are not homogenised (Sipiczki *et al.*, 2013; Sipiczki *et al.*, 2018). Because its ITS sequences do not fall into a single clade relative to the multiple ITS sequences of *M. fructicola* and *M. andauensis*, and because no genome sequence is available from the type strain of *M. pulcherrima*, strain APC 1.2 should properly be designated *M.* aff. *pulcherrima* rather than *M. pulcherrima*, but for convenience in the remainder of the text we use the latter name.

For competition assays, the filamentous fungi *Botrytis caroliniana* X.P. Li & Schnabel (isolate EC 1.05, SH177344.07FU), *Gibberella fujikuroi* ((Sawada) Wollenw.) (SH213620.07FU; isolate BC 8.14, CCOS1020) and *Fusarium oxysporum* f. sp. *radicis-lycopersici* (Schlecht as emended by Snyder and Hansen) (NRRL 26381/CL57 (ARS Culture Collection, USDA)) were used. The pigmentless mutant W8 (CCOS1866) was isolated from cells that were plated out after extended storage as freeze-dried powder at 22°C. All *M. pulcherrima* strains were maintained on potato dextrose agar (PDA; Becton, Dickinson and Company, Le Pont de Claix, France or Formedium™, Norfolk, United Kingdom) plates, grown at 22°C and transferred to fresh plates weekly.

Competition assays

The protocol for binary competition assays was based on the procedure by Hilber-Bodmer *et al.* (2017), but included minor adjustments. Yeasts cells and conidia of filamentous fungi were collected in water and adjusted to an OD_{600} of 0.001 and 0.1 respectively. Fifteen or 30 µl of the yeast suspension was plated on PDA plates of 5.5 or 9 cm diameter, respectively, and 5 µl of the conidial suspension were inoculated in the centre of the plates. Plates were incubated at 22°C for 3–15 days depending on the fungal species. Growth of the filamentous fungus was quantified before it reached the edge of the control plate (plate without yeasts) with the help of a planimeter (Planix 5, Tamaya Technics Inc., Tokyo, Japan). The average of the relative growth (growth in the presence of yeast/growth on control plate) of four replicates was calculated. All assays were repeated at least twice and showed comparable results.

For bioassays, conventionally grown cherries (1–2 weeks in cold storage) were washed with 70% ethanol and water, and a 2.5 mm wide and 3 mm deep lesion was created at the equator of each fruit using a custom-made tool. After complete drying of the lesion, 10 µl of a *M. pulcherrima* suspension (OD_{600} of 1) or sterile water as a control was applied to the lesion. After 3 h, 10 µl of a *Botrytis* conidia suspensions (10^5 conidia/ml) or water as a control was added to the lesions. The cherries of all treatments were kept on a dry filter paper in plastic trays, with a wet filter paper (soaked with 20 ml water) under the trays, and stored within a plastic bag at 22°C. After 4 days, rot and mycelium diameter were measured. For each treatment, 15 cherries were used and the experiment was performed twice for each treatment. The mean and standard errors of one representative experiment are shown.

Identification of secreted cyclic dipeptides

Twenty milliliter PDB containing 400 µl Amberlite XAD16N slurry (Sigma-Aldrich Chemie GmbH, Buchs, Switzerland) were inoculated with *M. pulcherrima* cells (wild-type, mutant, or complemented cells) to an OD_{600} of 0.1 and grown at 22°C for 2–3 days. For labelling experiments, yeast nitrogen base medium (without amino acids; Formedium™, Norfolk, United Kingdom) was prepared with $^{13}C_6$ D-Glucose (Cambridge Isotope Laboratories/ReseaChem GmbH, Burgdorf, Switzerland) and ammonium sulphate or with glucose and $^{15}N_2$ ammonium sulphate (Sigma-Aldrich Chemie GmbH, Buchs, Switzerland). The growth medium was discarded, the XAD beads were washed three times with water, and eluted with 1 ml methanol. The solvent was evaporated in a SpeedVac, the extracted material dissolved in 1 ml water, and the sample stored at –20°C until further analysis.

All extracts and a cyclo(Leu-Leu) standard (ChemFaces Biochemical Co., Ltd., Wuhan, China) were analysed by ultra-performance liquid chromatography-high resolution heated electrospray ionisation mass spectrometry (UPLC HR HESI-MS). Data were recorded on a Thermo Scientific™ Q Exactive™ Hybrid Quadrupole-Orbitrap Mass Spectrometer coupled to a Dionex Ultimate 3000 UPLC. We used the following solvent gradient (A = H_20 + 0.1% formic acid, B = acetonitrile + 0.1% formic acid with B 5–20% from 0–2 min, 20–98% from 2–20 min, 98% from 20–25 min, 98–5% from 25–27 min at a flowrate of 0.5 ml/min) on a Phenomenex Kinetex 2.6 µm XB-C18 100 Å (150 × 4.6 mm) column at 30°C. The MS was operated in positive ionisation mode at a scan range of 200–2000 m/*z* and a resolution of 70000. The spray voltage was set to 3.5 kV, the S-lens to 50, the auxiliary gas heater temperature to 438°C and the capillary temperature to 270°C. Further parameters used were AGC target (1e6), maximum injection time (200 ms), microscans (1), sheath gas (53), aux gas (14) and sweep gas (3).

Genome sequencing & mapping of mutations

Genomic DNA of the *M. pulcherrima* strain APC 1.2 was extracted using the Qiagen DNeasy Plant Mini Kit and sequenced on the PacBio RS II platform (performed at the Functional Genomics Center Zurich). Subsequent *de novo* genome assembly, polishing and resequencing were performed using PacBio SMRT Portal 2.3.0 (Stamatakis, 2014). The genomes of three mutant *M. pulcherrima* colonies (W8, W10 and W11) were sequenced using the Illumina MiSeq technology (Micro flow cell, paired-end, 250 bp), producing 1′225′187 W8, 1′087′938 W10 and 1′054′343 W11 reads. They were mapped to the *M. pulcherrima* reference genome using the BWA-MEM algorithm version 0.7.15. (Li, 2013). Secondary and supplementary alignments were removed subsequently using SAMtools (version 1.3.1) (Li *et al.*, 2009).

Genome annotation, phylogenetic analysis and functional characterisation

Genome annotation was performed using a modified version of the Yeast Genome Annotation Pipeline (YGAP; (Proux-Wera *et al.*, 2012)), which enabled to use the homology and synteny information from the *Candida* Gene Order Browser database instead of the Yeast Gene Order Browser database (CGOB and YGOB; (Maguire *et al.*, 2013, Byrne and Wolfe, 2005)). The CGOB database is composed of 13 species within the *Candida* (CUG-Ser1) clade, which are phylogenetically closer to *M. pulcherrima* than are the species in YGOB. YGAP was therefore modified to account for the alternative genetic code and to use a different ancestral reference for the synteny-based annotation. Because an ancestral gene order has not been yet inferred for the species in CGOB, the *Clavispora lusitanae* genome (Butler *et al.*, 2009) was used for synteny reference as it was found to be the closest relative to *M. pulcherrima* among the species in CGOB. The phylogenetic tree in Fig. 3A was constructed from an alignment of orthologous Snf2 proteins taken from CGOB, using MUSCLE, Gblocks and PhyML (1013 sites, GTR + gamma substitution model, 4 rate categories, 100 bootstrap replicates) as implemented in SeaView v4.50 (Gouy *et al.*, 2010) with their default parameters. The annotated genome of the wild-type *M. pulcherrima* strain APC 1.2 was functionally analysed and is being distributed by the Integrated Microbial Genomes (IMG) system of the Department of Energy's (DOE's) Joint Genome Institute (JGI) (IMG genome ID 2721755843; https://genome.jgi.doe.gov/portal/IMG_2721755843/IMG_2721755843.info.html) (Chen *et al.*, 2017). Chromosomes were numbered I to VII

from largest to smallest. Genes were given systematic names by YGAP such as *MPUL0C08850*, where *MPUL* indicates the species; 0 indicates the genome sequence version; *C* indicates chromosome III; *08850* is a sequential gene number counter that increments by 10 for each protein-coding gene and allow room for possible additions between genes. All loci, either predicted by YGAP or manually annotated, were deposited on NCBI using the METSCH_ locus tag and only those with functional annotation according to the JGI pipeline kept the *MPUL* prefix. The *M. pulcherrima* APC 1.2 genome is also available at NCBI under the BioProject PRJNA508581 (Accessions CP034456-CP034462 for the seven nuclear chromosomes).

RNAseq experiment

Wild-type and mutant (W8) *M. pulcherrima* cells were grown in potato dextrose broth (PDB; Formedium™, Norfolk, United Kingdom). An overnight culture was diluted with fresh medium to an OD_{600} of 0.4. After 5–6 h of growth at 23°C in a shaking incubator, 1 OD_{600} was collected, spun down, the supernatant was discarded, and the pellet frozen in liquid nitrogen and stored for later RNA extraction. Cells were mechanically disrupted with a FastPrep FP120 (speed 4.5, time 37 s; Thermo ELECTRON Corporation) and total RNA was extracted with the Qiagen RNeasy mini kit according to the manufacturers protocol and submitted for RNA sequencing to the Functional Genomics Center Zurich. RNA was quantified and verified with a Qubit® 3 fluorometer (Invitrogen) and a Bioanalyzer 2100 (Agilent, Waldbronn, Germany). The TruSeq Stranded mRNA Sample Prep Kit (Illumina, Inc, California, USA) was used for RNA depletion and reverse transcription of 1 μg of total RNA samples. The cDNA samples were fragmented, end-repaired and polyadenylated before ligation of TruSeq adapters for multiplexing. Fragments containing TruSeq adapters on both ends were selectively enriched with PCR. The quality and quantity of the enriched libraries were validated using Qubit® (1.0) Fluorometer and the Bioanalyzer 2100 (Agilent, Waldbronn, Germany). The TruSeq SR Cluster Kit v4-cBot-HS or TruSeq PE Cluster Kit v4-cBot-HS (Illumina, Inc, California, USA) was used for cluster generation using 8 pM of pooled normalised libraries on the cBOT. Sequencing was performed on the Illumina HiSeq 2500 paired-end at 2 X126 bp or single-end 126 bp using the TruSeq SBS Kit v4-HS (Illumina, Inc, California, USA). For the wild-type and the W8 mutant strain, two and three independent biological replicates were used for RNA extraction and consecutive sequencing respectively. The RNAseq data were analysed with an early version of the workflow available at https://github.com/csoneson/rnaseqworkflow. Briefly, reads were trimmed with TrimGalore! (https://www.bioinformatics.babraham.ac.uk/projects/trim_galore/) to remove adapters and low-quality sequences. Gene expression levels were estimated using Salmon (Patro *et al.*, 2017). To identify differentially expressed genes and estimate normalised expression values (counts per million), the counts were subsequently analysed with edgeR (69). The RNAseq data have been deposited in NCBI's Gene Expression Omnibus (Edgar *et al.*, 2002) and are accessible through GEO Series accession number GSE128386 (https://www.ncbi.nlm.nih.gov/geo/query/acc.cgi?acc=GSE128386).

Complementation of mutants

Wild-type and mutant *SNF2* coding sequences along with the flanking promoter and terminator sequences were PCR-amplified using Q5 High-fidelity polymerase (NEB) and primers 5′- caactagtAGTCAGCGTCACTTAGTGTGAAATACCTG and 5′-catgtcgacGTCCATCAATCGAATCAGCATAATACTGCC. Cycling conditions were as per manufacturer's instructions, with an annealing temperature of 64°C and an extension time of 3 min 15 s. Purified PCR products were ligated (T4 DNA ligase, NEB) via SpeI and SalI (NEB) restriction sites into a pEX-A2 plasmid backbone containing a codon-optimised nourseothricin (Nat, Werner Bioagents) yeast selection marker under the strong constitutive TEF promoter previously cloned from the *M. pulcherrima* genome. Ligations were used to transform competent *E.coli* (NEB, 5-alpha) with selection by ampicillin (Sigma, 100 μg/ml) and Nat (50 μg/ml). Positive colonies identified via colony PCR (DreamTaq Green PCR Mastermix, ThermoFisher; primers 5′-GCATGATGTGACTGTCGCCCGTAC and 5′-CCGTACTGGGCCTTGAGCTG; cycling conditions as per the manufacturer's instructions, with an annealing temperature of 59°C and an extension time of 1 min) were propagated overnight in Luria broth (Sigma) supplemented with 100 μg/ml ampicillin (Sigma) and 50 μg/ml Nat and plasmids purified via miniprep. All protocols used in the above cloning steps were as per the manufacturer's instructions and all purification steps performed using GeneJET kits (ThermoFisher).

Plasmids containing the WT or W8 mutant gene clone were digested with Acc65I and SalIHF (NEB) and used to transform both the WT and W8 *M. pulcherrima* strains using a lithium acetate method (Gietz and Woods, 2002). In brief, overnight cultures of the yeast strains were diluted to a starting OD_{600} of 0.3 and allowed to grow to an OD_{600} of 0.9. One millilitre of culture per transformation was centrifuged, the cell pellet washed once with PBS then resuspended in a transformation mix comprised of 800 μl 50% PEG-3350 + 100 μl 1M LiOAc pH 7.4 + 40 μl 5 mg/ml boiled salmon sperm + 100 μl 10XTE + 20 μl 1M DTT + 1 μg linearised plasmid. Transformations were incubated overnight (25°C, static), heat-shocked at 40°C for 5 min, placed on ice for 1 min then centrifuged for 5 min at 4000 rpm. The supernatant was removed, cells resuspended in 600 μl of SMB (30 g/l Tryptic Soy Broth (Sigma), 25 g/L Malt Extract (Sigma), pH 5) and incubated for 1 h (25°C, 200 rpm) before plating on to Malt Extract Agar (MEA, Sigma) plates containing 50 μg/ml Nat. After 2 days at 25°C, yeast colonies that grew were patched on to a second MEA + Nat plate. Colonies that grew overnight at 25°C were then subject to colony PCR to confirm the presence of the plasmid (primers and conditions as per colony PCR to confirm positive *E.coli* colonies above) and scored for colour (red or white).

Acknowledgements

Maja Hilber-Bodmer, Liesa Kunz, Chloé Douard, Andrea Knauf and Denise Müller are acknowledged for help with

experimental work. We are grateful to Prof. Mark Robinson (University of Zurich) and Dr. Charlotte Soneson (Friedrich Miescher Institute for Biomedical Research, Basel) for access to an early version of their RNASeq data analysis workflow. Michael Schmid helped with genome assembly. The project is supported by the Swiss National Science Foundation (SNSF, grant 31003A_175665/1) to FMF. DGL and MMB are funded by the Industrial Biotechnology Catalyst (Innovate UK, BBSRC, EPSRC) to support the translation, development and commercialisation of innovative Industrial Biotechnology processes (EP/N013522/1).

Author contributions

Responsibilities for the different methods and sections of the manuscript was shared as follows: DGL, MMB and DH established the transformation protocol for *M. pulcherrima* and generated the complemented strains. KHW and RAOM annotated and analysed the *M. pulcherrima* genome and *SNF2* gene. KS, VS and CHA sequenced and assembled the *M. pulcherrima* genome, identified the *snf2* point mutation, and analysed the RNAseq experiment. AB and JP performed the UPLC HR HESI-MS analyses and thus identified cyclo(Leu-Leu), pulcherriminic acid and the precursors and degradation products of these compounds. IS, MS, PK, ASK and MPRM performed all competition assays, growth experiments and grew the cultures for DNA, RNA and metabolite analyses. FMF isolated the pigmentless mutants, analysed *PUL* gene transcription, coordinated the study and wrote the majority of the manuscript. All authors have read and agree with the manuscript.

Data Availability Statement

The annotated genome of the wild-type *M. pulcherrima* strain APC 1.2 is being distributed by the Integrated Microbial Genomes (IMG) system of the Department of Energy's (DOE's) Joint Genome Institute (JGI) (IMG genome ID 2721755843; https://genome.jgi.doe.gov/portal/IMG_2721755843/IMG_2721755843.info.html) and is also available at NCBI under the BioProject PRJNA508581 (Accessions CP034456-CP034462 for the seven nuclear chromosomes). The RNAseq data are accessible through GEO Series accession number GSE128386 (https://www.ncbi.nlm.nih.gov/geo/query/acc.cgi?acc=GSE128386).

References

Abarenkov, K., Nilsson, R.H., Larsson, K.H., Alexander, I.J., Eberhardt, U., Erland, S., *et al.* (2010) The UNITE database for molecular identification of fungi – recent updates and future perspectives. *New Phytologist*, **186**, 281–285.

Agaimy, A. and Foulkes, W.D. (2018) Hereditary SWI/SNF complex deficiency syndromes. *Seminars in Diagnostic Pathology*, **35**, 193–198.

Banani, H., Spadaro, D., Zhang, D., Matic, S., Garibaldi, A. and Gullino, M.L. (2014) Biocontrol activity of an alkaline serine protease from *Aureobasidium pullulans* expressed in *Pichia pastoris* against four postharvest pathogens on apple. *International Journal of Food Microbiology*, **182–183**, 1–8.

Bar-Shimon, M., Yehuda, H., Cohen, L., Weiss, B., Kobeshnikov, A., Daus, A., *et al.* (2004) Characterization of extracellular lytic enzymes produced by the yeast biocontrol agent *Candida oleophila*. *Current Genetics*, **45**, 140–148.

Biegel, J.A., Busse, T.M. and Weissman, B.E. (2014) SWI/SNF chromatin remodeling complexes and cancer. *American Journal of Medical Genetics Part C: Seminars in Medical Genetics*, **166C**, 350–366.

Butler, G., Rasmussen, M.D., Lin, M.F., Santos, M.A., Sakthikumar, S., Munro, C.A., *et al.* (2009) Evolution of pathogenicity and sexual reproduction in eight *Candida* genomes. *Nature*, **459**, 657–662.

Byrne, K.P. and Wolfe, K.H. (2005) The yeast gene order browser: combining curated homology and syntenic context reveals gene fate in polyploid species. *Genome Research*, **15**, 1456–1461.

Carlson, M., Osmond, B.C. and Botstein, D. (1981) Mutants of yeast defective in sucrose utilization. *Genetics*, **98**, 25–40.

Chai, B., Huang, J., Cairns, B.R. and Laurent, B.C. (2005) Distinct roles for the RSC and Swi/Snf ATP-dependent chromatin remodelers in DNA double-strand break repair. *Genes & Development*, **19**, 1656–1661.

Chantasuban, T., Santomauro, F., Gore-Lloyd, D., Parsons, S., Henk, D., Scott Roderick, J. and Chuck, C. (2018) Elevated production of the aromatic fragrance molecule, 2-phenylethanol, using *Metschnikowia pulcherrima* through both de novo and ex novo conversion in batch and continuous modes. *Journal of Chemical Technology and Biotechnology*, **93**, 2118–2130.

Chen, I.A., Markowitz, V.M., Chu, K., Palaniappan, K., Szeto, E., Pillay, M., *et al.* (2017) IMG/M: integrated genome and metagenome comparative data analysis system. *Nucleic Acids Research*, **45**, D507–D516.

Contreras, A., Hidalgo, C., Henschke, P.A., Chambers, P.J., Curtin, C. and Varela, C. (2014) Evaluation of non-*Saccharomyces* yeasts for the reduction of alcohol content in wine. *Applied and Environment Microbiology*, **80**, 1670–1678.

Contreras, A., Curtin, C. and Varela, C. (2015) Yeast population dynamics reveal a potential 'collaboration' between *Metschnikowia pulcherrima* and *Saccharomyces uvarum* for the production of reduced alcohol wines during Shiraz fermentation. *Applied Microbiology and Biotechnology*, **99**, 1885–1895.

Cook, A.H. and Slater, C.A. (1954) Metabolism of 'wild' yeasts. I. The chemical nature of pulcherrimin. *Journal of the Institute of Brewing*, **60**, 213–217.

Cryle, M.J., Bell, S.G. and Schlichting, I. (2010) Structural and biochemical characterization of the cytochrome P450 CypX (CYP134A1) from *Bacillus subtilis*: a cyclo-L-leucyl-L-leucyl dipeptide oxidase. *Biochemistry*, **49**, 7282–7296.

De Curtis, F., de Felice, D.V., Ianiri, G., De Cicco, V. and Castoria, R. (2012) Environmental factors affect the activity

of biocontrol agents against ochratoxigenic *Aspergillus carbonarius* on wine grape. *International Journal of Food Microbiology*, **159**, 17–24.
Dudley, A.M., Janse, D.M., Tanay, A., Shamir, R. and Church, G.M. (2005) A global view of pleiotropy and phenotypically derived gene function in yeast. *Molecular Systems Biology*, **1**, E1–E11.
Dutta, A., Sardiu, M., Gogol, M., Gilmore, J., Zhang, D., Florens, L., *et al.* (2017) Composition and function of mutant Swi/Snf complexes. *Cell Reports*, **18**, 2124–2134.
Edgar, R., Domrachev, M. and Lash, A.E. (2002) Gene Expression Omnibus: NCBI gene expression and hybridization array data repository. *Nucleic Acids Research*, **30**, 207–210.
Enyenihi, A.H. and Saunders, W.S. (2003) Large-scale functional genomic analysis of sporulation and meiosis in *Saccharomyces cerevisiae*. *Genetics*, **163**, 47–54.
Gietz, R.D. and Woods, R.A. (2002) Transformation of yeast by lithium acetate/single-stranded carrier DNA/polyethylene glycol method. *Methods in Enzymology*, **350**, 87–96.
Gondry, M., Sauguet, L., Belin, P., Thai, R., Amouroux, R., Tellier, C., *et al.* (2009) Cyclodipeptide synthases are a family of tRNA-dependent peptide bond-forming enzymes. *Nature Chemical Biology*, **5**, 414–420.
Gouy, M., Guindon, S. and Gascuel, O. (2010) SeaView version 4: a multiplatform graphical user interface for sequence alignment and phylogenetic tree building. *Molecular Biology and Evolution*, **27**, 221–224.
Gross, S., Kunz, L., Muller, D.C., Santos Kron, A. and Freimoser, F.M. (2018) Characterization of antagonistic yeasts for biocontrol applications on apples or in soil by quantitative analyses of synthetic yeast communities. *Yeast*, **35**, 559–566.
Hilber-Bodmer, M., Schmid, M., Ahrens, C.H. and Freimoser, F.M. (2017) Competition assays and physiological experiments of soil and phyllosphere yeasts identify *Candida subhashii* as a novel antagonist of filamentous fungi. *BMC Microbiology*, **17**, 4.
Janisiewicz, W.J., Tworkoski, T.J. and Kurtzman, C.P. (2001) Biocontrol potential of *Metchnikowia pulcherrima* strains against blue mold of apple. *Phytopathology*, **91**, 1098–1108.
Kántor, A., Hutková, J., Petrová, J., Hleba, L. and Kacániová, M. (2015) Antimicrobial activity of pulcherrimin pigment produced by *Metschnikowia pulcherrima* against various yeast species. *Journal of Microbiology, Biotechnology and Food Sciences*, **5**, 282–285.
Kluyver, A.J., Vanderwalt, J.P. and Vantriet, A.J. (1953) Pulcherrimin, the pigment of *Candida pulcherrima*. *Proceedings of the National Academy of Sciences*, **39**, 583–593.
Koren, S., Walenz, B.P., Berlin, K., Miller, J.R., Bergman, N.H. and Phillippy, A.M. (2017) Canu: scalable and accurate long-read assembly via adaptive k-mer weighting and repeat separation. *Genome Research*, **27**, 722–736.
Krause, D.J., Kominek, J., Opulente, D.A., Shen, X.-X., Zhou, X., Langdon, Q.K., *et al.* (2018) Functional and evolutionary characterization of a secondary metabolite gene cluster in budding yeasts. *Proceedings of the National Academy of Sciences*, **115**(43), 11030–11035.
Kupfer, D.G., Uffen, R.L. and Canale-Parola, E. (1967) The role of iron and molecular oxygen in pulcherrimin synthesis by bacteria. *Archiv für Mikrobiologie*, **56**, 9–21.
Laur, J., Ramakrishnan, G.B., Labbe, C., Lefebvre, F., Spanu, P.D. and Belanger, R.R. (2018) Effectors involved in fungal-fungal interaction lead to a rare phenomenon of hyperbiotrophy in the tritrophic system biocontrol agent-powdery mildew-plant. *New Phytologist*, **217**, 713–725.
Laurent, B.C., Treich, I. and Carlson, M. (1993a) Role of yeast SNF and SWI proteins in transcriptional activation. *Cold Spring Harbor Symposia on Quantitative Biology*, **58**, 257–263.
Laurent, B.C., Treich, I. and Carlson, M. (1993b) The yeast SNF2/SWI2 protein has DNA-stimulated ATPase activity required for transcriptional activation. *Genes & Development*, **7**, 583–591.
Leverentz, B., Conway, W.S., Janisiewicz, W., Abadias, M., Kurtzman, C.P. and Camp, M.J. (2006) Biocontrol of the food-borne pathogens Listeria monocytogenes and Salmonella enterica serovar Poona on fresh-cut apples with naturally occurring bacterial and yeast antagonists. *Applied and Environment Microbiology*, **72**, 1135–1140.
Li, H. (2013) Aligning sequence reads, clone sequences and assembly contigs with BWA-MEM. arXiv:1303.3997v2.
Li, X., Wang, D., Cai, D., Zhan, Y., Wang, Q. and Chen, S. (2017) Identification and high-level production of pulcherrimin in *Bacillus licheniformis* DW2. *Applied Biochemistry and Biotechnology*, **183**, 1323–1335.
Li, H., Handsaker, B., Wysoker, A., Fennell, T., Ruan, J., Homer, N., *et al.* (2009) The sequence alignment/map format and SAMtools. *Bioinformatics*, **25**, 2078–2079.
Liu, X., Li, M., Xia, X., Li, X. and Chen, Z. (2017) Mechanism of chromatin remodelling revealed by the Snf2-nucleosome structure. *Nature*, **544**, 440–445.
MacDonald, J.C. (1963) The structure of pulcherriminic acid. *Canadian Journal of Chemistry*, **41**, 165–172.
MacDonald, J.C. (1965) Biosynthesis of pulcherriminic acid. *The Biochemical Journal*, **96**, 533–538.
Maguire, S.L., OhEigeartaigh, S.S., Byrne, K.P., Schroder, M.S., O'Gaora, P., Wolfe, K.H. and Butler, G. (2013) Comparative genome analysis and gene finding in *Candida* species using CGOB. *Molecular Biology and Evolution*, **30**, 1281–1291.
Melvydas, V., Staneviciene, R., Balynaite, A., Vaiciuniene, J. and Garjonyte, R. (2016) Formation of self-organized periodic patterns around yeasts secreting a precursor of a red pigment. *Microbiological Research*, **193**, 87–93.
Mulleder, M., Calvani, E., Alam, M.T., Wang, R.K., Eckerstorfer, F., Zelezniak, A. and Ralser, M. (2016) Functional metabolomics describes the yeast biosynthetic regulome. *Cell*, **167**(553–565), e512.
Neigeborn, L. and Carlson, M. (1984) Genes affecting the regulation of *SUC2* gene expression by glucose repression in *Saccharomyces cerevisiae*. *Genetics*, **108**, 845–858.

Nilsson, R.H., Larsson, K.H., Taylor, A.F.S., Bengtsson-Palme, J., Jeppesen, T.S., Schigel, D., *et al.* (2018) The UNITE database for molecular identification of fungi: handling dark taxa and parallel taxonomic classifications. *Nucleic Acids Research*, **47**(D1), D259–D264.

Orij, R., Urbanus, M.L., Vizeacoumar, F.J., Giaever, G., Boone, C., Nislow, C., *et al.* (2012) Genome-wide analysis of intracellular pH reveals quantitative control of cell division rate by pH(c) in *Saccharomyces cerevisiae*. *Genome Biology*, **13**, R80.

Oro, L., Ciani, M. and Comitini, F. (2014) Antimicrobial activity of *Metschnikowia pulcherrima* on wine yeasts. *Journal of Applied Microbiology*, **116**, 1209–1217.

Ortiz-Merino, R.A., Varela, J.A., Coughlan, A.Y., Hoshida, H., da Silveira, W.B., Wilde, C., *et al.* (2018) Ploidy variation in *Kluyveromyces marxianus* separates dairy and non-dairy isolates. *Front Genet*, **9**, 94.

Parafati, L., Vitale, A., Restuccia, C. and Cirvilleri, G. (2015) Biocontrol ability and action mechanism of food-isolated yeast strains against *Botrytis cinerea* causing post-harvest bunch rot of table grape. *Food Microbiology*, **47**, 85–92.

Patro, R., Duggal, G., Love, M.I., Irizarry, R.A. and Kingsford, C. (2017) Salmon provides fast and bias-aware quantification of transcript expression. *Nature Methods*, **14**, 417–419.

Pelliccia, C., Antonielli, L., Corte, L., Bagnetti, A., Fatichenti, F. and Cardinali, G. (2011) Preliminary prospection of the yeast biodiversity on apple and pear surfaces from Northern Italy orchards. *Annals of Microbiology*, **61**, 965–972.

Peterson, C.L. and Tamkun, J.W. (1995) The SWI-SNF complex: a chromatin remodeling machine? *Trends in Biochemical Sciences*, **20**, 143–146.

Piano, S., Neyrotti, V., Migheli, Q. and Gullino, M.L. (1997) Biocontrol capability of *Metschnikowia pulcherrima* against *Botrytis* postharvest rot of apple. *Postharvest Biology and Technology*, **11**, 131–140.

Piombo, E., Sela, N., Wisniewski, M., Hoffmann, M., Gullino, M.L., Allard, M.W., *et al.* (2018) Genome sequence, assembly and characterization of two *Metschnikowia fructicola* strains used as biocontrol agents of postharvest diseases. *Frontiers in Microbiology*, **9**, 593.

Prasad, P., Lennartsson, A. and Ekwall, K. (2015) The roles of SNF2/SWI2 nucleosome remodeling enzymes in blood cell differentiation and leukemia. *BioMed Research International*, **2015**, 347571.

Proux-Wera, E., Armisen, D., Byrne, K.P. and Wolfe, K.H. (2012) A pipeline for automated annotation of yeast genome sequences by a conserved-synteny approach. *BMC Bioinformatics*, **13**, 237.

Randazzo, P., Aubert-Frambourg, A., Guillot, A. and Auger, S. (2016) The MarR-like protein PchR (YvmB) regulates expression of genes involved in pulcherriminic acid biosynthesis and in the initiation of sporulation in *Bacillus subtilis*. *BMC Microbiology*, **16**, 190.

Reddy, K.R., Spadaro, D., Gullino, M.L. and Garibaldi, A. (2011) Potential of two *Metschnikowia pulcherrima* (yeast) strains for *in vitro* biodegradation of patulin. *Journal of Food Protection*, **74**, 154–156.

Riley, R., Haridas, S., Wolfe, K.H., Lopes, M.R., Hittinger, C.T., Goker, M., *et al.* (2016) Comparative genomics of biotechnologically important yeasts. *Proceedings of the National Academy of Sciences*, **113**, 9882–9887.

Ruiz-Moyano, S., Martin, A., Villalobos, M.C., Calle, A., Serradilla, M.J., Cordoba, M.G. and Hernandez, A. (2016) Yeasts isolated from figs (*Ficus carica* L.) as biocontrol agents of postharvest fruit diseases. *Food Microbiology*, **57**, 45–53.

Santamauro, F., Whiffin, F.M., Scott, R.J. and Chuck, C.J. (2014) Low-cost lipid production by an oleaginous yeast cultured in non-sterile conditions using model waste resources. *Biotechnology for Biofuels*, **7**, 34.

Saravanakumar, D., Clavorella, A., Spadaro, D., Garibaldi, A. and Gullino, M.L. (2008) *Metschnikowia pulcherrima* strain MACH1 outcompetes *Botrytis cinerea*, *Alternaria alternata* and *Penicillium expansum* in apples through iron depletion. *Postharvest Biology and Technology*, **49**, 121–128.

Serviene, E., Luksa, J., Orentaite, I., Lafontaine, D.L. and Urbonavicius, J. (2012) Screening the budding yeast genome reveals unique factors affecting K2 toxin susceptibility. *PLoS ONE*, **7**, e50779.

Sipiczki, M. (2006) *Metschnikowia* strains isolated from botrytized grapes antagonize fungal and bacterial growth by iron depletion. *Applied and Environmental Microbiology*, **72**, 6716–6724.

Sipiczki, M., Pfliegler, W.P. and Holb, I.J. (2013) *Metschnikowia* species share a pool of diverse rRNA genes differing in regions that determine hairpin-Loop structures and evolve by reticulation. *PLoS ONE*, **8**, e67384.

Sipiczki, M., Horvath, E. and Pfliegler, W.P. (2018) Birth-and-death evolution and reticulation of ITS segments of *Metschnikowia andauensis* and *Metschnikowia fructicola* rDNA repeats. *Frontiers in Microbiology*, **9**, 1193.

Slavikova, E., Vadkertiova, R. and Vranova, D. (2007) Yeasts colonizing the leaf surfaces. *Journal of Basic Microbiology*, **47**, 344–350.

Spadaro, D., Vola, R., Piano, S. and Gullino, M.L. (2002) Mechanisms of action and efficacy of four isolates of the yeast *Metschnikowia pulcherrima* active against postharvest pathogens on apples. *Postharvest Biology and Technology*, **24**, 123–134.

Stamatakis, A. (2014) RAxML version 8: a tool for phylogenetic analysis and post-analysis of large phylogenies. *Bioinformatics*, **30**, 1312–1313.

Stern, M., Jensen, R. and Herskowitz, I. (1984) Five SWI genes are required for expression of the HO gene in yeast. *Journal of Molecular Biology*, **178**, 853–868.

Tang, M.R., Sternberg, D., Behr, R.K.Sloma, A. and Berka, R. (2006) Use of transcriptional profiling & bioinformatics to solve production problems: eliminating red pigment production in a *Bacillus subtilis* strain producing hyaluronic acid. *Industrial Biotechnology*, **2**, 66–74.

Turkel, S., Korukluoglu, M. and Yavuz, M. (2014) Biocontrol activity of the local strain of *Metschnikowia pulcherrima* on different postharvest pathogens. *Biotechnology Research International*, **2014**, 397167.

Uffen, R.L. and Canale-Parola, E. (1972) Synthesis of pulcherriminic acid by *Bacillus subtilis*. *Journal of Bacteriology*, **111**, 86–93.

Vadkertiova, R., Molnarova, J., Vranova, D. and Slavikova, E. (2012) Yeasts and yeast-like organisms associated with fruits and blossoms of different fruit trees. *Canadian Journal of Microbiology*, **58**, 1344–1352.

Venkatesh, A., Murray, A.L., Boyle, A.B., Quinn Farrington, L., Maher, T.J., O'Gaora, P., *et al.* (2018) Draft genome sequence of a highly heterozygous yeast strain from the *Metschnikowia pulcherrima* subclade, UCD127. *Genome Announc*, **6**, e00550-18.

Wang, D., Zhan, Y., Cai, D., Li, X., Wang, Q. and Chen, S. (2018) Regulation of the synthesis and secretion of the iron chelator cyclodipeptide pulcherriminic acid in *Bacillus licheniformis*. *Applied and Environment Microbiology*, **84**, e00262-00218.

Wilson, B.G. and Roberts, C.W. (2011) SWI/SNF nucleosome remodellers and cancer. *Nature Reviews Cancer*, **11**, 481–492.

Supporting Information

Additional supporting information may be found online in the Supporting Information section at the end of the article